New Findings on the Diels−Alder Reactions. An Analysis Based on the Bonding Evolution Theory

Slawomir Berski,*,† Juan Andrés,*,‡ Bernard Silvi,§ and Luis R. Domingo#

Faculty of Chemistry, University of Wroclaw, F. Joliot-Curie 14, 50-383, Wroclaw, Poland, Departament de Ciències Experimentals, Universitat Jaume I, Apartat 224, 12080, Castelló, Spain, Laboratoire de Chimie Théorique, Université Pierre et Marie Curie, 4 Place Jussieu, 75252 Paris Cedex, France, and Instituto de Ciencia Molecular, Departamento de Química Orgánica, Universidad de Valencia, Dr. Moliner 50, 46100 Burjassot, Valencia, Spain

Received: July 5, 2006

Two Diels−Alder type reactions, i.e., normal electron demand (NED) between 1,3-butadiene (**BD**) and acrolein (**Acr**) and inverse electron demand (IED) between 2,4-pentadienal (**PDA**) and methyl vinyl ether (**MVE**), have been investigated using the bonding evolution theory (BET). BET combines topological analysis of the electron localization function (ELF) and catastrophe theory. Catalyst effect has been incorporated through Lewis acid BH_3. The B3LYP hybrid HF/DFT method along with 6-31G(d), 6-311++G(d,p) basis sets have been used. All reactions yield two-stage mechanism and there is no topological evidence that they might be concerted with two bonds partially formed during transition structure. A formation of six-membered ring requires 10 (or 11) steps separated by two types of catastrophes: fold and cusp. The first "intermolecular" bond (C_1-C_6) is formed at 1.93, 1.92 Å (NED) and 1.92, 1.97 Å (IED). The six-membered ring is "closed" at 2.11, 2.13 Å (NED) and 2.5, 2.6 Å (IED) via formation of the second bond C_4-C_5. All reactions begin with "reduction" of C=C bonds to single C−C (cusp catastrophes). Subsequently, the nonbonding electron density is concentrated (fold catastrophes) on terminal C atoms. Finally the new bonds, C_1-C_6 and C_4-C_5, are established (cusp catastrophes). Both magnitude and regularity of the electron redistribution, happening during reactions enable us to distinguish two effects: (1) the "ring effect", where a large amount of electron density is regularly transferred from double C=C bonds to intermolecular regions and single C−C bonds, (2) the "side chain effect"—usually weaker and irregular—involving substituents' bonds. In the transition structure, well formed bonding basin $V(C_1,C_6)$, is observed only for the **PDA**$\cdots BH_3$/**MVE** reaction. For other reactions only the nonbonding basins: $V(C_1)$ and $V(C_6)$, are found in the interaction region $C_1\cdots C_6$.

I. Introduction

Chemistry is a study of bond making/forming processes and understanding how reactants convert into products, via the transition state (TS) and possible intermediates. Contemporary determination of principles controlling reaction mechanisms is closely tied with progress of quantum chemistry. One of the fundamental goals for a given chemical rearrangement is to analyze changes of quantum mechanical observables along the reaction pathway, using first principle calculations. This approach enables a comprehensive picture of the chemical reactivity in terms of how and when the chemical events, bond breaking/forming processes, will emerge.

Bonding evolution theory (BET)[1] combines topological analysis of the electron localization function (ELF)[2] and Thom's catastrophe theory.[3] This proved to be an appropriate tool for organic reactions studies, particularly the reorganization of electron pairing during the reaction course. We have recently studied molecular mechanism for several chemical reactions: between ethylene (**Eth**) and 1,3-butadiene (**BD**),[4] the 1,3 dipolar reaction between fulminic acid and acetylene,[5] the Bergman reaction,[6] the ethylene trimerization to yield benzene[7] and the Cope reaction.[8] The reaction pathway can be established using intrinsic reaction coordinate (IRC) procedure[9] on the potential energy surface. This enables electron density reorganization analysis, occurring during reaction, in terms of the bond forming/breaking processes.

The DA reaction is the classic example of chemical transformation in organic chemistry and is widely used in synthetic organic chemistry for the construction of six-membered rings.[10−16] This justifies the development of theoretical models for DA reactions, involving a large number of dienes and dienophiles. Therefore, considerable attention has been paid to molecular mechanism elucidation.[17−21] In particular, the DA reaction between (ethylene) **Eth** and (1,3-buthadiene) **BD** yielding to cyclohexadiene is often taken as the classic example of a pericyclic reaction.[22,23] Despite its apparent simplicity, the reaction mechanism nature is controversial and therefore subject of numerous experimental and theoretical studies.[22−26] The concerted nature of the mechanism and its stereospecificity have been established and are now well understood,[12,18,22] although a stepwise mechanism involving biradical intermediates can coexist.[22,25]

To explain the cycloadduct regiochemistry and DA reaction stereoselectivity, the frontier molecular orbital (FMO) theory[26] is applied. In this approach chemical reactivity is controlled by both the highest occupied molecular orbital (HOMO) and the

* Corresponding authors. E-mail: sberski@wchuwr.chem.uni.wroc.pl (S.B.); andres@exp.uji.es (J.A.).
† University of Wroclaw.
‡ Universitat Jaume I.
§ Université Pierre et Marie Curie.
# Universidad de Valencia.

10.1021/jp068071t CCC: $33.50
Published on Web 12/07/2006

lowest unoccupied molecular orbital (LUMO). The prototype reaction between **Eth** and **BD** is, however, not the typical laboratory case. The DA reaction requires opposite electronic arrangements at the diene/dienophile pair for being reasonably fast. If one considers frontier orbital relative energies for diene and dienophile systems, the DA reactions can be divided into two limiting categories: (1) the normal electron demand (NED) DA reaction, $HOMO_{diene}-LUMO_{dienophile}$ controlled, and (2) the inverse electron demand (IED) type, in which the energy gap between $HOMO_{dienophile}$ and $LUMO_{diene}$ governs the reaction rate. The NED is activated by an energy gap decrease between the HOMO of the electron-rich diene and the LUMO of the electron-poor dienophile, whereas the IED type reaction is favored by electron-poor dienes with very low LUMOs and an electron-rich dienophile with a high HOMO. To activate the NED-DA reaction dienophiles, the electron-withdrawing groups should be used, as these will lower the LUMO energy, increasing reactivity. To increase the NED reaction activation further, Lewis acid (LA) catalysis should be applied to lower the $LUMO_{dienophile}$ energy even more. Thus a more favorable interaction with the $HOMO_{diene}$ will be possible. The IED reaction can also be catalyzed by LA and/or electron-withdrawing groups at the diene fragment. In both cases, the charge-transfer process goes from the electron-rich reactant to the electron-poor one at the corresponding TS. It allows preferential polar TS stabilization and causes further reduction in the activation energy.[27] A large change in charge separation can occur on the way from reactants to the TS, and the process becomes concerted but highly asynchronous.[25,27−29] It also may proceed through a stepwise pathway along a zwitterionic intermediate.[30,31] Under suitable conditions, the stepwise process intermediate can be trapped.[32] Therefore, NED-DA and IED-DA reactions are favored by opposite substituent properties on diene and dienophile fragments.

To understand the bonding trend along the reaction pathways for different types of formal DA rearrangements and to gain an insight into nature of TS, the combination of ELF and catastrophe theory have been used. Molecular mechanism studies of two NED-DA reactions have been performed. They included the reaction between **BD** and acrolein (**Acr**) and the reaction of **BD** and **Acr** coordinated with BH_3 modeling a LA catalyst, $CH_2{=}CH-CH{=}CH_2/CH_2{=}CH-CHO(\cdots BH_3)$. Additionally, investigations of the IED-DA reactions' molecular mechanisms have been undertaken, namely between 2,4-pentadienal (**PDA**) and methyl vinyl ether (**MVE**) and of **PDA** coordinated with BH_3 and **MVE**, $CH_2{=}CH-CH{=}CH-CHO(\cdots BH_3)/CH{=}CH-OCH_3$.

This strategy allows characterization of the reaction pathway through optimized geometries and ELF topologies for corresponding stationary points on the IRC path. Thus, useful information about reactivity can be derived from comparative analysis.

The paper is arranged as follows. Section II analyses and discusses obtained results. Conclusions are presented in section III. In the Supporting Information, some computational details are summarized (S1). The catastrophe theory and the ELF topological analysis are presented in S2 and S3, respectively.

II. Results and Discussion

Lewis type formulas, revealed by BET, and representing bonding in different steps on the IRC path are shown in Figures 1, 3, 5 and 7. We were unable to localize first catastrophe at $r(C_1\cdots C_6) > 2.87$ Å, $r(C_4\cdots C_5) > 3.16$ Å for reaction III and at $r(C_1\cdots C_6) > 2.97$ Å, $r(C_4\cdots C_5) > 3.41$ Å for reaction IV. A

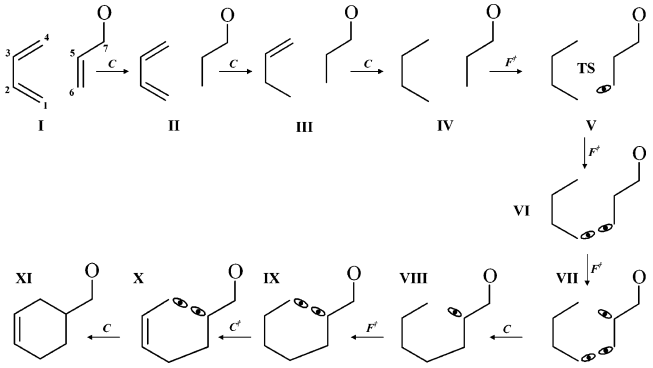

Figure 1. Lewis type formula representing bonding in different steps on the IRC path of the reaction between 1,3-butadiene and acrolein revealed by the bonding evolution theory (BET).

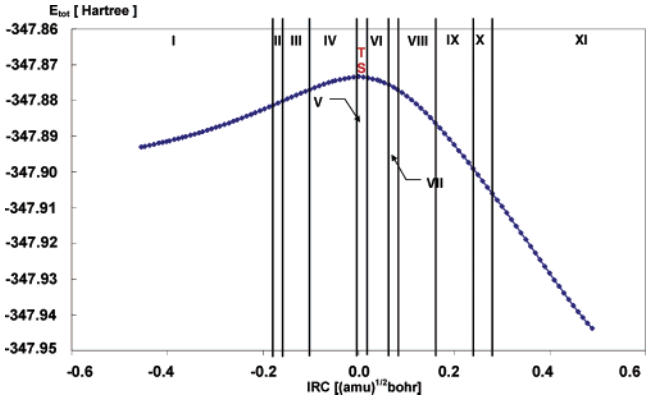

Figure 2. Fragment of the intrinsic reaction coordinate (IRC) curve for the reaction between 1,3-butadiene and acrolein with marked domains of the structural stability.

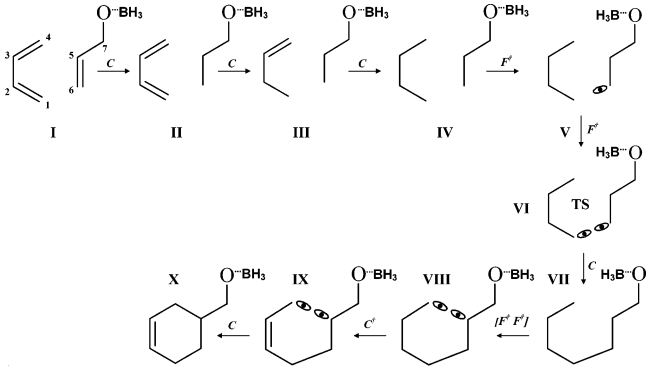

Figure 3. Lewis type formula representing bonding in different steps on the IRC path of the reaction between 1,3-butadiene and acrolein catalyzed by BH_3 revealed by the bonding evolution theory (BET).

comparison of ELF topologies of the reactants for isolated forms and second step revealed that first catastrophe is of the cusp type. In **PDA** two disynaptic basins $V_1(C_3,C_4)$ and $V_2(C_3,C_4)$ are merged into a singular basin $V_{1\cup2}(C_3,C_4)$—the double $C_3{=}C_4$ bond is "reduced" to the single bond C_3-C_4. Figures 2, 4, 6 and 8 show IRC curve fragments for the above reactions with domains of structural stability marked. The interatomic $r(C_1\cdots C_6)$, $r(C_4\cdots C_5)$ distances and basin populations ($\bar{N}$) for different points on the IRC path, for both the NED-DA and IED-DA reactions, are presented in Tables 1−4. The data are related to **BD**/**Acr**, **BD**/**Acr**$\cdots BH_3$ and **PDA**/**MVE**, **PDA**$\cdots BH_3$/**MVE** reactions.

All investigated NED-DA and IED-DA reactions can be represented by chemical equations where the arrow symbol is replaced by the more informative catastrophe sequence (see

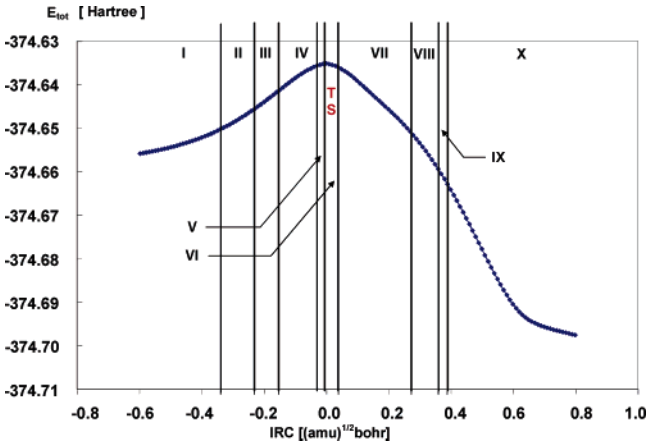

Figure 4. Fragment of the intrinsic reaction coordinate (IRC) curve for the reaction between 1,3-butadiene and acrolein catalyzed by BH_3 with marked domains of the structural stability.

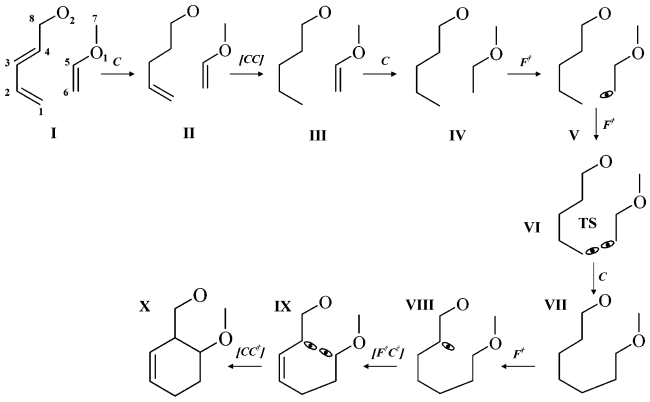

Figure 5. Lewis type formula representing bonding in different steps on the IRC path of the reaction between 2,4-pentadienal and methyl vinyl ether revealed by the bonding evolution theory (BET). The catastrophes occurring in the same point on the IRC path, when one bifurcation leads to merging and separation of two $V_1(O_1)$ and $V_2(O_1)$ basins, are presented as *[CC]* and *[CC†]*.

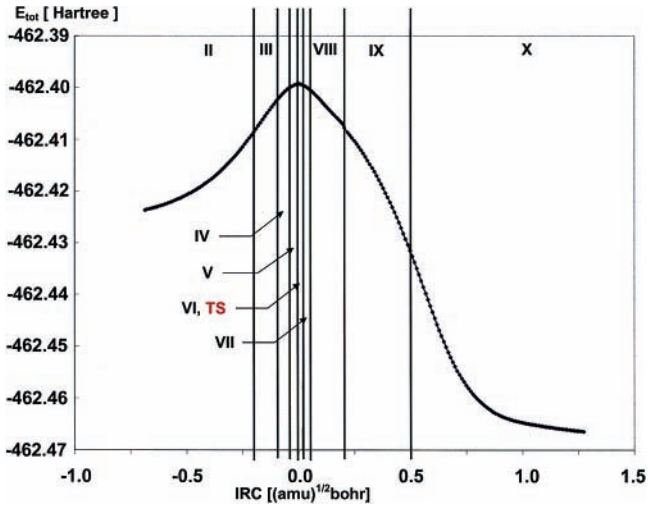

Figure 6. Fragment of the Intrinsic Reaction Coordinate (IRC) curve for the reaction between 2,4-pentadienal and methyl vinyl ether with marked domains of the structural stability.

Supporting Information): "N_2-*FCSHEBP*···-N_3" where N_2 is a number of the domains of structural stability, "*FCS*···" are symbols of the catastrophes and $N_3 = 0$ denotes the reaction end (the sequence of catastrophes). In our case, *C* and *F* refer to the cusp and fold catastrophes and *[CF]* denotes two

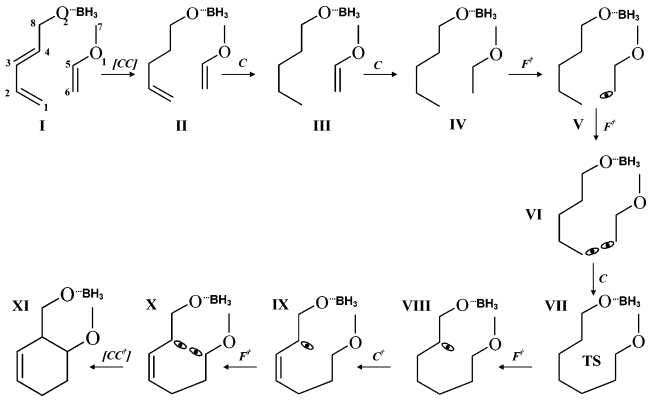

Figure 7. Lewis type formula representing bonding in different steps on the IRC path of the reaction between 2,4-pentadienal and methyl vinyl ether catalyzed by BH_3 revealed by the bonding evolution theory (BET). The catastrophes occurring in the same point on the IRC path, when one bifurcation leads to merging and separation of two $V_1(O_1)$ and $V_2(O_1)$ basins, are presented as *[CC]* and *[CC†]*.

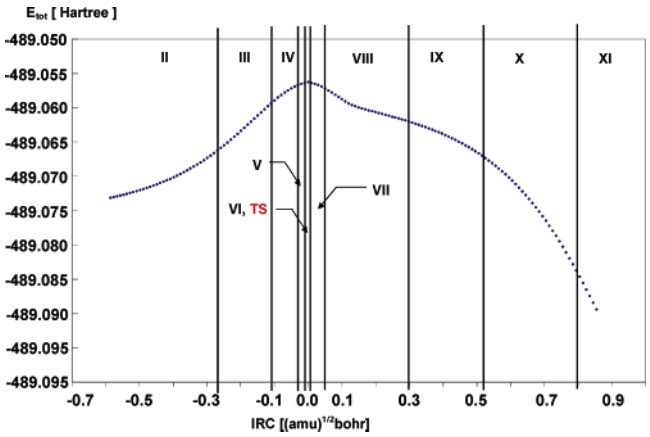

Figure 8. Fragment of the intrinsic reaction coordinate (IRC) curve for the reaction between 2,4-pentadienal and methyl-vinyl ether catalyzed by BH_3 with marked domains of the structural stability.

catastrophes occurring simultaneously or observed at the same point on the IRC path though not related by symmetry.

$C_4H_6 + C_2H_4$:

7-*[CC]C[F†F†][F†F†][**CC**]C†*-0: C_6H_{10}

$C_4H_6 + C_2H_3CHO$:

11-*CCCF†F†F†**C**F†C†C*-0: C_6H_9CHO

$C_4H_6 + C_2H_3CHO\cdots BH_3$:

10-*CCCF†F†**C**[F†F†]C†C*-0: $C_6H_9CHO\cdots BH_3$

$C_4H_5CHO + C_2H_3OCH_3$:

10-*C[CC]CF†F†**C**F†[F†C†][CC†]*-0: $C_6H_8OCH_3CHO$

$C_4H_5CHO\cdots BH_3 + C_2H_3OCH_3$:

11-*[CC]CCF†F†**C**F†C†F†[CC†]*-0: $C_6H_8OCH_3CHO\cdots BH_3$

Furthermore, $C^\dagger$ ($F^\dagger$) is the cusp (fold) catastrophe, which leads to a basin number increase and *C* (*F*) is the cusp (fold), which decreases the number of basins. Bold ***C*** stands for the cusp catastrophe leading to first intermolecular bond formation (C_1−C_6). We compared our results with those obtained before for reaction between **BD** and **Eth**.[4]

TABLE 1: Interatomic Distances, Basin Populations [e] and Types of the Catastrophes Computed for Different Points on the IRC Path of the Reaction between 1,3-Butadiene (BD) and Acrolein (Acr)[a]

basin	step I **BD**	step I **Acr**	step II	step III	step IV	step V TS	step VI	step VII	step VIII	step IX	step X	step XI **CA1**	XI min **CA1**
$r(C_1\cdots C_6)$			2.414	2.381	2.286	2.091	2.055	1.964	1.933	1.804	1.694	1.653	1.536
$r(C_4\cdots C_5)$			2.722	2.699	2.638	2.521	2.500	2.444	2.423	2.326	2.205	2.134	1.547
$V_1(C_1,C_2)$	1.73		1.70	3.29	3.23	3.14	2.75	2.52	2.44	2.25	2.14	2.11	2.00
$V_2(C_1,C_2)$	1.72		1.59										
$V_1(C_2,C_3)$	2.26		2.33	2.36	2.41	2.65	2.72	2.93	3.00	3.23	1.84	1.88	1.81
$V_2(C_2,C_3)$											1.55	1.55	1.80
$V_1(C_3,C_4)$	1.73		1.74	1.74	3.28	3.15	3.10	2.98	2.95	2.54	2.34	2.27	2.01
$V_2(C_3,C_4)$	1.72		1.60	1.59									
$V(C_1)$							0.35	0.52					
$V(C_4)$							-	-		0.30	0.45		
$V(C_5)$							-	0.26	0.28	0.43	0.54		
$V(C_6)$						0.27	0.34	0.49					
$V(C_1,C_6)$									1.08	1.38	1.59	1.65	1.89
$V(C_4,C_5)$												1.11	1.85
$V_1(C_5,C_6)$		1.67	3.30	3.28	3.28	2.87	2.75	2.55	2.48	2.25	2.11	2.08	1.90
$V_2(C_5,C_6)$		1.78											
$V(C_5,C_7)$		2.25	2.33	2.31	2.36	2.50	2.56	2.40	2.41	2.39	2.32	2.30	2.11
$V(C_7,O)$		2.35	2.32	2.33	2.33	2.31	2.31	2.31	2.31	2.31	2.33	2.34	2.43
$V_1(O)$		2.56	2.63	2.63	2.64	2.65	2.64	2.64	2.66	2.65	2.64	2.64	2.59
$V_2(O)$		2.58	2.59	2.59	2.59	2.60	2.61	2.61	2.62	2.60	2.59	2.59	2.52
catastrophe			*C*	*C*	*C*	$F^{\dagger}$	$F^{\dagger}$	$F^{\dagger}$	***C***	$F^{\dagger}$	$C^{\dagger}$	*C*	

[a] The intermolecular distances (Å) correspond to first point after the catastrophe. The calculations are carried out with the 6-31G(d) basis set. **CA1** = cyclohex-3-enecarbaldehyde.

TABLE 2: Interatomic Distances, Basin Populations [e] and Types of the Catastrophes Calculated for Different Points on the IRC Path of the Reaction between 1,3-Butadiene (BD) and Acrolein (Acr) Catalyzed by BH_3[a]

basin	step I **BD**	step I **Acr**$\cdots$**BH$_3$**	step II	step III	step IV	step V	step VI TS	step VII	step VIII	step IX	step X **CA1**$\cdots$**BH$_3$**	step X min **CA1**$\cdots$**BH$_3$**
$r(C_1\cdots C_6)$			2.625	2.444	2.319	2.071	2.032	1.916	1.611	1.587	1.581	1.534
$r(C_4\cdots C_5)$			3.032	2.926	2.863	2.759	2.744	2.697	2.355	2.178	2.118	1.548
$V_1(C_1,C_2)$	1.69		1.66	3.00	3.15	3.08	2.78	2.57	2.14	2.10	2.08	2.04
$V_2(C_1,C_2)$	1.69		1.54									
$V_1(C_2,C_3)$	2.23		2.29	2.34	2.38	2.55	2.60	2.74	3.21	1.77	1.84	1.76
$V_2(C_2,C_3)$										1.52	1.48	1.77
$V_1(C_3,C_4)$	1.69		1.70	1.72	3.21	3.08	3.04	2.94	2.57	2.32	2.28	2.02
$V_2(C_3,C_4)$	1.69		1.54	1.51								
$V(C_1)$							0.29					
$V(C_4)$									0.17	0.33		
$V(C_5)$									0.32	0.48		
$V(C_6)$						0.17	0.23					
$V(C_1,C_6)$								0.97	1.64	1.69	1.70	1.88
$V(C_4,C_5)$											0.92	1.84
$V_1(C_5,C_6)$		1.61	3.15	3.15	3.13	2.86	2.81	2.58	2.16	2.09	2.08	1.82
$V_2(C_5,C_6)$		1.61										
$V(C_5,C_7)$		2.34	2.42	2.45	2.50	2.63	2.65	2.76	2.65	2.48	2.44	2.16
$V(C_7,O)$		2.37	2.31	2.28	2.28	2.23	2.21	2.16	2.16	2.23	2.26	2.46
$V_1(O)$		2.94	3.03	3.00	3.04	3.11	3.11	3.15	3.14	3.11	3.10	2.88
$V_2(O)$		2.16	2.16	2.19	2.17	2.13	2.15	2.15	2.17	2.16	2.16	2.15
catastrophe			*C*	*C*	*C*	$F^{\dagger}$	$F^{\dagger}$	***C***	$F^{\dagger}F^{\dagger}$	$C^{\dagger}$	*C*	

[a] The intermolecular distances (Å) correspond to first after the catastrophe. The calculations are carried out with the 6-311+G(d,p) basis set. **CA1** = cyclohex-3-enecarbaldehyde.

For the DA reactions only two types of catastrophes are observed, namely the fold and cusp. A formation of the nonbonding basin $V(C_i)$ is achieved by the fold $[F^{\dagger}]$. The cusp leads from single C_i-C_j to double $C_i=C_j$ bonds breaking/formation $[C]/[C^{\dagger}]$. Except for the first reaction, which due to concerted synchronous mechanism consists only of 7 steps, other reactions exhibit 10 or 11 steps. In the NED-DA reaction, **BD**/**Acr**$\cdots$$BH_3$, two catastrophes occur at the same point on the IRC path, i.e., $[F^{\dagger}F^{\dagger}]$ between the steps VII and VIII (Figure 3). In the IED-DA reaction, **PDA**/**MVE**, the cusp and fold $[F^{\dagger}C^{\dagger}]$ are observed between steps VIII and IX (Figure 5) at the end of the reaction. These results, however, could be related to the grid quality and should be treated with a caution. Furthermore, in the initial step of the **PDA**/**MVE** and **PDA**$\cdots$$BH_3$/**MVE** reactions, the cusp merges nonbonding $V_1(O_1)$ and $V_2(O_1)$ basins $[C]$ into a single basin $V_{1\cup2}(O_1)$, whereas at the end both reactions present a splitting $[C^{\dagger}]$ of $V_{1\cup2}(O_1)$ into well separated $V_1(O_1)$ and $V_2(O_1)$. Both catastrophes reflect electron density redistributions for oxygen lone electron pairs associated with the ELF change. These catastrophes are included into the catastrophe sequences as $[CC]$ and $[CC^{\dagger}]$.

There is a considerable difference between the NED- and IED-DA reactions at the second step of the reaction. In the NED-DA, the $C_5=C_6$ bond (**Acr**) is "reduced" first, whereas in IED-DA first "reduction" is observed for the double $C_3=C_4$ bond (**PDA**). In both NED- and IED-DA there is no double bond $C_2=C_3$ formation in the last step as was observed in the **BD**/**Eth** reaction. However, formation of the $C_2=C_3$ bond happens in step IX or X, before the C_4-C_5 bond is established.

TABLE 3: Intermolecular Distances, Basin Populations [e] and Types of the Catastrophes Calculated for Different Points on the IRC Path of the Reaction between 2,4-Pentadienal (PDA) and Methyl Vinyl Ether (MVE)[a]

basin	step I **PDA**	step I **MVE**	step II	step III	step IV	step V	step VI TS	step VII	step VIII	step IX **CA2**	step X **CA2**	step X min **CA2**
$r(C_1\cdots C_6)$			2.868	2.399	2.164	2.084	2.024	1.923	1.864	1.637	1.566	1.536
$r(C_4\cdots C_5)$			3.155	2.972	2.900	2.877	2.859	2.826	2.805	2.601	2.016	1.547
$V_1(C_1,C_2)$	1.78		1.72	3.27	3.20	3.14	2.90	2.50	2.38	2.13	2.05	2.01
$V_2(C_1,C_2)$	1.65		1.63									
$V_1(C_2,C_3)$	2.27		2.32	2.40	2.53	2.65	2.71	3.08	3.16	1.67	1.75	1.82
$V_2(C_2,C_3)$										1.76	1.82	1.83
$V_1(C_3,C_4)$	1.76		3.33	3.27	3.24	3.20	3.19	3.12	2.79	2.47	2.13	2.01
$V_2(C_3,C_4)$	1.61											
$V(C_4,C_8)$	2.31		2.34	2.37	2.38	2.42	2.41	2.42	2.42	2.41	2.19	2.05
$V(C_8,O_2)$	2.35		2.32	2.30	2.27	2.26	2.25	2.26	2.24	2.24	2.37	2.43
$V_1(O_2)$	2.56		2.59	2.58	2.61	2.62	2.62	2.64	2.65	2.65	2.05	2.47
$V_2(O_2)$	2.63		2.63	2.65	2.67	2.67	2.68	2.65	2.66	2.66	2.65	2.44
$V(C_1)$							0.23					
$V(C_4)$									0.32	0.53		
$V(C_1,C_6)$								1.05	1.18	1.62	1.80	1.88
$V(C_4,C_5)$											1.58	1.94
$V(C_5)$										0.28		
$V(C_6)$						0.38	0.50					
$V_1(C_5,C_6)$		1.87	1.82	1.82	3.48	3.10	2.96	2.82	2.73	2.32	2.07	1.99
$V_2(C_5,C_6)$		1.87	1.85	1.75								
$V(C_5,O_1)$		1.47	1.51	1.53	1.59	1.60	1.62	1.64	1.66	1.67	1.46	1.28
$V(C_7,O_1)$		1.29	1.30	1.33	1.34	1.34	1.35	1.37	1.38	1.38	1.31	1.28
$V_1(O_1)$		2.35	2.41	4.56	4.51	4.48	4.43	4.41	4.38	4.36	2.61	2.57
$V_2(O_1)$		2.35	2.24								2.60	2.54
catastrophe			*C*	*C C*	*C*	$F^{\dagger}$	$F^{\dagger}$	***C***	$F^{\dagger}$	$F^{\dagger}C^{\dagger}$	*C* $C^{\dagger}$	

[a] The intermolecular distances (Å) correspond to first point after the catastrophe. In the step II first point analyzed by BET is presented. **CA2** = 6-methoxycyclohex-2-enecarbaldehyde.

TABLE 4: Intermolecular Distances, Basin Populations [e] and Types of the Catastrophes Calculated for Different Points on the IRC Path of the Reaction between 2,4-Pentadienal (PDA) and Methyl Vinyl Ether (MVE) Catalyzed by BH_3 (MVE)[a]

basin	step I **PDA···BH_3**	step I **MVE**	step II	step III	step IV	step V	step VI	step VII TS	step VIII	step IX	step X	step XI **CA2···BH_3**	step XI min **CA2···BH_3**
$r(C_1\cdots C_6)$			2.963	2.544	2.216	2.075	2.034	1.971	1.867	1.633	1.598	1.561	1.530
$r(C_4\cdots C_5)$			3.404	3.248	3.166	3.138	3.130	3.118	3.095	2.812	2.492	2.003	1.550
$V_1(C_1,C_2)$	1.74		1.70	3.22	3.11	3.04	2.83	2.54	2.37	2.11	2.06	2.01	1.99
$V_2(C_1,C_2)$	1.63		1.58										
$V_1(C_2,C_3)$	2.28		2.29	2.37	2.53	2.67	2.72	2.98	3.12	1.68	1.67	1.74	1.77
$V_2(C_2,C_3)$										1.70	1.77	1.79	1.81
$V_1(C_3,C_4)$	1.67		3.16	3.15	3.11	3.06	3.04	3.00	2.72	2.42	2.29	2.10	1.97
$V_2(C_3,C_4)$	1.59												
$V(C_4,C_8)$	2.42		2.44	2.47	2.54	2.57	2.59	2.61	2.65	2.69	2.54	2.30	2.41
$V(C_8,O_2)$	2.28		2.23	2.21	2.16	2.14	2.13	2.11	2.10	2.08	2.13	2.28	2.08
$V_1(O_2)$	3.02		3.11	3.15	3.18	3.22	3.24	3.26	3.28	3.28	3.23	3.05	2.95
$V_2(O_2)$	2.21		2.17	2.15	2.16	2.16	2.16	2.15	2.14	2.15	2.16	2.18	2.15
$V(C_1)$							0.19						
$V(C_4)$									0.21	0.39	0.56		
$V(C_1,C_6)$								0.83	1.08	1.55	1.65	1.77	1.86
$V(C_4,C_5)$												1.43	1.89
$V(C_5)$											0.20		
$V(C_6)$						0.38	0.45						
$V_1(C_5,C_6)$		1.87	1.80	1.73	3.40	3.00	2.92	2.83	2.68	2.37	2.25	2.05	1.96
$V_2(C_5,C_6)$		1.87	1.81	1.78									
$V(C_5,O_1)$		1.47	1.51	1.54	1.61	1.68	1.68	1.72	1.76	1.83	1.72	1.51	1.28
$V(C_7,O_1)$		1.29	1.31	1.33	1.34	1.36	1.37	1.37	1.39	1.41	1.39	1.34	1.25
$V_1(O_1)$		2.35	4.65	4.59	4.45	4.41	4.39	4.34	4.28	4.19	4.34	4.61	2.50
$V_2(O_1)$		2.35											2.41
catastrophe			*C C*	*C*	*C*	$F^{\dagger}$	$F^{\dagger}$	***C***	$F^{\dagger}$	$C^{\dagger}$	$F^{\dagger}$	*C* $C^{\dagger}$	

[a] The intermolecular distances (Å) correspond to first point after the catastrophe. In the step II first point analyzed by BET is presented. **CA2** = 6-metoxycyclohex-2-enecarbaldehyde.

On the basis of the BET methodology, all reactions undergo three distinctive phases: (1) a "double $C_i{=}C_j$ bonds reduction" to single $C_i{-}C_j$ bonds (*CCC* sequence), (2) a nonbonding electron density concentration on atoms forming new bonds ($F^{\dagger}F^{\dagger}F^{\dagger}F^{\dagger}$ sequence), (3) a formation of new covalent bonds $C_1{-}C_6$, $C_4{-}C_5$, (***CC***), and (4) a single $C_2{-}C_3$ bond transformation to double $C_2{=}C_3$ bond ($C^{\dagger}$).

As indicated by the catastrophe sequences, an order of different steps may vary; however, the reactions begin always with three cusp catastrophes *(CCC)*, leading to double $C_i{=}C_j$ "reduction" to single $C_i{-}C_j$ bonds and a formation of the nonbonding basins on the C_1, C_6 atoms by 2-fold bifurcations ($F^{\dagger}F^{\dagger}$). The three cusp catastrophes are consequence of the electron density redistribution to the $C_1\cdots C_6$ and $C_4\cdots C_5$ regions (electron

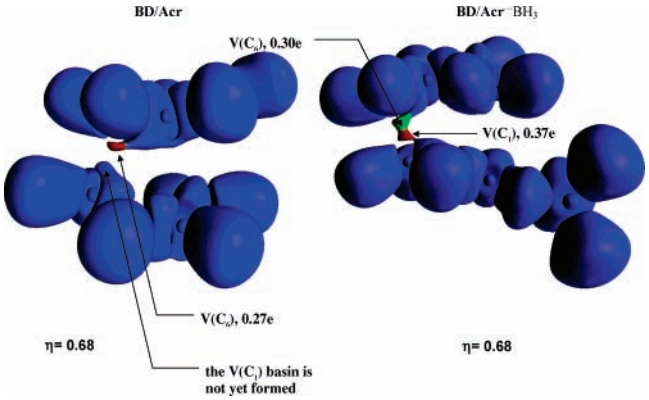

Figure 9. Electron localization function ($\eta = 0.68$) plots for the transition state of the reactions between 1,3-butadiene and acrolein uncatalyzed and catalyzed by BH_3.

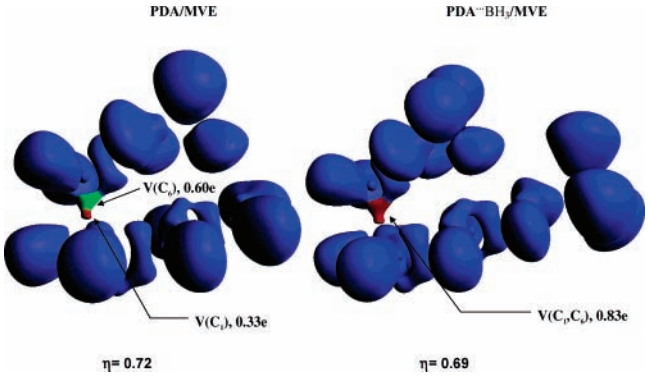

Figure 10. Electron localization function ($\eta = 0.68$) plots for the transition state of the reactions between 2,4-pentadienal and methylvinyl ether uncatalyzed and catalyzed by BH_3.

density delocalization). From the classical point of view one can discuss two stage mechanisms where the C_1-C_6 and C_4-C_5 bonds are formed at different points on the IRC path.

Comparison of the IRC paths (Figures 2, 4 and 6, 8) with marked domains of the structural stability reveals the first and the last steps to be the longest. This can be explained as a result of large electron density redistribution and an electron localization properties' change to fulfill first catastrophe conditions or to minimize total energy in the last step. In the IED-DA reactions a number of points in consecutive domains decrease when one goes to TS. This effect, however, is not observed for the NED-DA reactions. A step comprising TS is very short and can usually be found only for 2−3 points on the IRC path. A length of other steps depends on the reaction studied.

The BET enables us to show exact distances at which new intermolecular bonds C_1-C_6 and C_4-C_5 are established. However, one has to be conscious that, in a point following the respective catastrophe, new bonds are yet not entirely formed because saturation with the electron density is finished later, usually in the last step (the energy minimum). For the NED-DA reactions, the C_1-C_6 bond is formed at ca. 1.93 (I) and 1.92 Å (II). For the IED-DA reactions III and IV, it is formed at ca. 1.92 and 1.97 Å, respectively. A formation of the second bond C_4-C_5 occurs at ca. 2.13 (I), 2.12 Å (II) and 2.02 (III), 2.00(IV) Å.

In this paper, an effect of the catalyst (BH_3) using ELF topological analysis combined with the catastrophe theory is explained for the first time. A presence of the catalyst yields qualitative effect and events on the reaction path are changed. In the case of the NED-DA reaction, **BD**/**Acr**···BH_3, a "construction" of the C_1-C_6 bond in TS, with two $V(C_1)$ and $V(C_6)$ basins, is more advanced (Figure 9) than for the uncatalyzed **BD**/**Acr** reaction with only one $V(C_1)$ basin. Similarly for the IED-DA reaction, **PDA**/**MVE**, there are two basins, $V(C_1)$ and $V(C_6)$, in TS but one can see the already formed C_1-C_6 bond with bonding $V(C_1,C_6)$ basin for the catalyzed reaction **PDA**···BH_3/**MVE** (Figure 10).

Population analysis of $V(C_1,C_6)$ and $V(C_4,C_5)$ basins, at points following the cusp catastrophes, shows a catalyst effect. For the **BD**/**Acr** and **PDA**/**MVE** reactions, electron density in the $V(C_1,C_6)$ basin (1.08e and 1.05e) is larger than in the presence of BH_3 for the **BD**/**Acr**···BH_3 and **PDA**···BH_3/**MVE** reactions (0.97e and 0.83e). Qualitatively similar results are achieved for the second C_4-C_5 bond with 1.11e, 1.58e for **BD**/**Acr**, **PDA**/**MVE** and 0.92e, 1.43e for **BD**/**Acr**···BH_3, **PDA**···BH_3/MVE. It therefore becomes apparent that in the presence of the catalyst, the chemical bond is formed at lower electron density concentrations. It displays an electron pairing enhancement in the interaction region.

Basin populations computed for different points on the IRC path for the NED-DA (Tables 1 and 2) and IED-DA reactions (Tables 3 and 4) reveal redistribution of electron density. Owing to its magnitude and direction one can distinguish the "ring effect" and "side chain effect". To follow a synchronous concerted mechanism in the reaction between **BD** and **Eth**, where the reactants are without substituents, the electron flux is simple. In BD, this occurs from the $C_1=C_2$, $C_3=C_4$ double bonds to the C_2-C_3 bond and intermolecular $C_1\cdots C_6$, $C_4\cdots C_5$ regions. In **Eth**, electron flux is observed from the $C_5=C_6$ bond to the $C_1\cdots C_6$, $C_4\cdots C_5$ regions. Such redistribution of the electron density in the six-membered ring is called the "ring effect". When reactants are substituted, a picture becomes more complicated because the electron density is redistributed also to the bonds outside the ring. This usually weak effect is called "side chain effect".

In the **BD**/**Acr** reaction the "ring effect" yields large electron flux in **BD**. This occurs from the $V_{1\cup2}(C_1,C_2)$ and $V_{1\cup2}(C_3,C_4)$ basins to $V(C_2,C_3)$ and intermolecular regions $C_1\cdots C_6$ and $C_4\cdots C_5$. During the reaction the respective basin populations are decreased by 1.45e and 1.44e and $V(C_2,C_3)$ is increased by 1.35e. This implies that about 1.5e is transferred to the $C_1\cdots C_6$ and $C_4\cdots C_5$ regions. In **Acr** 1.55e flows from $V(C_5,C_6)$ to the $C_1\cdots C_6$ and $C_4\cdots C_5$ regions. As can be seen from Table 1, observed changes are very regular. The "side chain effect" is relatively small and the C_5-C_7 bond in **Acr** alters irregularly from 2.25e to 2.11e with a maximum of 2.56e in the sixth step. Other bonds present less significant changes, around 0.1e. For **BD**/**Acr**···BH_3 reaction the "side chain effect" is stronger. The C_5-C_7 bond in **Acr** alters its basin population in an irregular mode from 2.34e to 2.16e with a maximum of 2.76e (step VII) and the C_7-O bond from 2.37e to 2.46e with a minimum of 2.16e (step VII and VIII). Furthermore, BH_3 polarizes one of the lone electron pairs $V_1(O)$ increasing its population from 2.94e to 3.15e (step VII) and decreasing to 2.88e (energy minimum). A magnitude of the "ring effect" can be compared to the one observed for the **BD**/**Acr** reaction though the electron flux in both reactants is about 0.1e smaller.

The IED-DA reactions yield strong both "ring effect" and "side chain effect". In the **PDA**/**MVE** reaction electron flux within six-membered ring is regular with a transfer of about 1.4e in **PDA** from the $V(C_1,C_2)$ and $V(C_3,C_4)$ basins to $V(C_2,C_3)$ and 1.8e depopulation of $V(C_5,C_6)$ in **MVE**. This can be associated with an electron-releasing effect of the OCH_3 group. A magnitude of the "side chain effect" in the **MVE** is similar to one found for the **BD**/**Acr** reaction and the population of the

C_5-O_1, C_7-O_1 bonds changes by about 0.4e and 0.1e, respectively, with maximum in the step IX. The main difference between the **BD/Acr** and **PDA/MVE** reactions is reflected in dramatic changes in the oxygen lone electron pairs in **MVE**, which justifies a characterization of the "side chain effect" as "strong". During the reaction the population of $V_1(O)$ and $V_2(O)$ changes from about 4.7e to 5.11e with a maximum of 5.2e at a beginning of the step X and a minimum of 4.36e in the step IX. This irregular electron density redistribution is reflected in the ELF-topology and for $r(C_1\cdots C_6)$ and $r(C_4\cdots C_5)$ of ca. 2.40 and 2.97 Å the $V_1(O_1)$ and $V_2(O_1)$ basins are joined by the cusp catastrophe (step III) into singular basin $V_{1\cup 2}(O_1)$. Such ELF-topology is retained until a C_4-C_5 bond formation (step IX) when the second cusp catastrophe recovers two $V_1(O_1)$ and $V_2(O_1)$ basins (step X). In the **PDA**$\cdots BH_3$/**MVE** reaction, a magnitude of the "ring effect" is slightly smaller than observed for **PDA/MVE**. The "side chain effect" reveals irregular change of $V(C_5,O_1)$ and $V(C_7,O_1)$ population with maximum in step IX. The electron-withdrawing LA molecule effectively polarizes the oxygen lone electron pairs resulting in the cusp catastrophes in the step II and step XI (energy minimum).

Birney and Houk[33] emphasized that the DA reactions are, in general, concerted with both bonds partially formed at the transition state. Recently, it has been suggested that substitution on the diene and dienophile favors the charge transfer along with an asynchronous mechanism.[34] To answer the question of whether the intermolecular bonds are really formed in TS, one can analyze an ELF topology in respective steps. In the reaction between **Eth** and **BD** (archetypal DA reaction) TS was found in the step III where all $C_i{=}C_j$ bonds are "reduced" to single bonds without any indication of C_1-C_6 and C_4-C_5 bond formation. A substitution on **Eth** with an aldehyde group to obtain **Acr** alters electronic features. **Acr** is expected to act as an electrophile and **BD** as a nucleophile, and net charge transfer would take place from the diene toward the dienophile. The TS is observed in step V where the nonbonding basin $V(C_6)$ appears on the carbon atom of **Acr**. In the case of the **BD/Acr**$\cdots BH_3$ reaction, a more polar mechanism is expected with the charge-transfer enhancement. The TS (step VI) is characterized by two nonbonding basins $V(C_1)$ and $V(C_6)$ localized in **Acr**. Figure 9 presents ELF distributions ($\eta = 0.68$) for both reactions. For **BD/Acr** reaction one observes singular nonbonding basin $V(C_6)$ (red color) and a small region with increased electron pairing on C_1 atom subsequently forming the $V(C_1)$ basin. In the **BD/Acr**$\cdots BH_3$ reaction both monosynaptic basins $V(C_1)$ and $V(C_6)$ are already formed. However, to be able to compare our results with the experimental ones, it is necessary to stress that on the basis of topological analysis there are two possibilities: (1) the A−B bond is formed at the same time when the V(A,B) bonding basin is identified by BET (the catastrophe theory is very precise thus the moment of bond formation is exact) and (2) the A−B bond can be "partially formed" for all points on the IRC when the nonbonding V(A) and V(B) basins are already created but not yet merged into V(A,B), thus before the respective cusp catastrophe. In light of statement 1, it needs to be emphasized that the C_1-C_6 and C_4-C_5 bonds are not formed in TS. It supports the hypothesis that the **BD/Acr** and **BD/Acr**$\cdots BH_3$ reactions follow a two-stage mechanism, in which the C_1-C_6 bond is formed first. However, assuming statement 2, a partially formed bond C_1-C_6 is observed in TS only for the catalyzed reaction **BD/Acr**$\cdots BH_3$.

In the case of the IED-DA reactions the situation is different. There is an electron-withdrawing substituent (the CHO group)

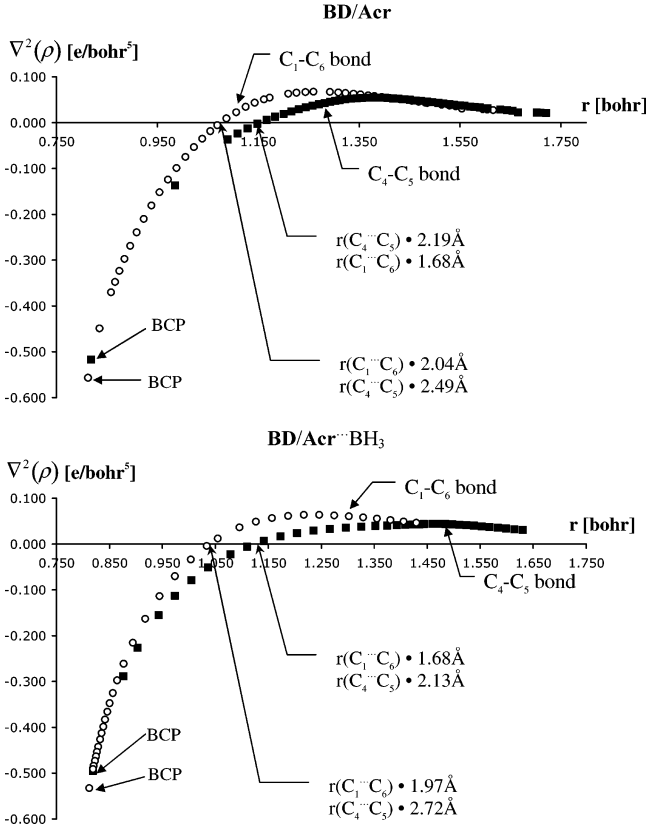

Figure 11. Change of the Laplacian of the electron density $\nabla^2(\rho(\mathbf{r}))$ for the critical point of index 1 localized between C_1, C_6 and C_4, C_5 atoms for selected points on the IRC path in the reaction between 1,3-butadiene and acrolein.

on the diene and an electron-releasing substituent (the OCH_3 group) on the dienophile. As can be seen from Figure 10 ($\eta = 0.72$ and 0.69), for the **PDA/MVE** reaction TS (sixth step) exhibits two well-formed nonbonding basins $V(C_1)$ and $V(C_6)$ denoted in red and green (for **MVE**). A small region of increased electron pairing on the C_4 atom (**PDA**) is also observed, this will results in forming the $V(C_4)$ basin in the eighth step. In **PDA**$\cdots BH_3$/**MVE** the new C_1-C_6 bond (red color) in TS (seventh step) is already established via the $V(C_1,C_6)$ basin. This is an exception among investigated reactions. It is worthwhile to emphasize that, similarly to the NED-DA reactions, there is no significiant proof that the second C_4-C_5 bond is formed in TS, even in light of the statement 2. ELF analysis does not support the concept of asynchronous TS.

In the framework of the atoms in molecules (AIM) method developed by Bader,[35] the electron density Laplacian $\nabla^2(\rho)$ calculated for the critical point of index 1 ((3,−1)), lying on the gradient path joining two nuclear attractors, indicates the nature of chemical bond. When a molecule has a minimal energy, such a point is called the bond critical point (BCP). The shared-electron bonds correspond to $\nabla^2(\rho) < 0$ whereas ionic bonds (dominated by the electrostatic interactions) are characterized by $\nabla^2(\rho) > 0$. The electron density Laplacian is a measure of electron density concentration around the BCP. Figure 11 shows an analysis of $\nabla^2(\rho)$ values for the critical point of index 1, localized between C_1,C_6 and C_4,C_5 atoms for the IRC path in the **BD/Acr** reaction. As the interpretation of BCP is constrained only to the energy minimum, we refer to a measure of electron density concentration. In the energy minima when the reactions are terminated, $\nabla^2(\rho)$ values for BCPs are less than zero (covalent interactions) and comparable because the differences between the C_1-C_6 and C_4-C_5 bonds are small.

TABLE 5: Topological Data for the Localization Basins Involved in a Formation of the C_1-C_6 and C_4-C_5 Intermolecular Bonds in TS for All Studied Reactions[a]

basin Ω	$\bar{N}$ [e]	σ^2	λ	cov(Ω_i,Ω_j)
			BD/Acr	
$V(C_6)$	0.27	0.24	0.91	$0.05V(C_5,C_6)$
			BD/Acr···BH_3	
$V(C_1)$	0.37	0.32	0.88	$0.07V(C_1,C_2)$
$V(C_6)$	0.30	0.27	0.90	$0.05V(C_5,C_6)$, $0.04V(H_8,C_6)$, $0.04V(H_9,C_6)$
			PDA/MVE	
$V(C_1)$	0.33	0.29	0.89	$0.05V(C_1,C_2)$, $0.04V(H_1,C_1)$, $0.04V(H_2,C_1)$
$V(C_6)$	0.60	0.49	0.82	$0.11V(C_1)$
			PDA···BH_3/MVE	
$V(C_1,C_6)$	0.83	0.63	0.76	$0.12V(C_5,C_6)$, 0.08, $V(C_1,C_2)$

[a] $\bar{N}$ = the basin population. σ^2 = the variance of the basin population. λ = the relative fluctuation. cov(Ω_i, Ω_j) = the covariance of the basin population.

At the beginning of both reactions, $\nabla^2(\rho)$ values are larger than 0 because a mutual interaction between the reactants leads to an electron cloud overlap and an increase of the kinetic energy over the potential energy contribution. For the C_1-C_6 bond in the **BD/Acr** reaction $\nabla^2(\rho)$ changes sign at 2.04 Å ($r(C_4\cdots C_5)$ = 2.49 Å) and for the C_4-C_5 bond at 2.19 Å ($r(C_1\cdots C_6)$ = 1.68 Å). One can notice that in the case of the C_1-C_6 bond a beginning of electron density concentration around the (3,−1) critical point is close to TS, i.e., $r(C_1\cdots C_6)$ = 2.091 Å, $r(C_4\cdots C_5)$ = 2.522 Å; however, it is not true for the C_4-C_5 bond. Similar results are obtained for the **BD/Acr**···BH_3 reaction, where $\nabla^2(\rho)$ for the C_1-C_6 bond changes sign at 1.97 Å, being rather close to TS (1.993 Å). These results support our hypothesis of two stage mechanism for the DA reactions, forming the C_1-C_6 bond as the first one and in TS proximity.

Table 5 gathers the topological data computed for selected basins in TS. Population analysis for newly formed basins shows the value of 0.27e for $V(C_6)$ in the **BD**/**Acr** reaction, 0.37e for $V(C_1)$, 0.30e for $V(C_6)$ in **BD**/**Acr**···BH_3, 0.33e and 0.60e for $V(C_1)$ and $V(C_6)$ in **PDA**/**MVE**, 0.83e for $V(C_1,C_6)$ in **PDA**···BH_3/**MVE**. Electron density delocalization in the monosynaptic basins is very large (σ^2 = 0.24−0.49) and the relative fluctuation λ ranges between 0.82 and 0.91. Covariance contributions analysis presents a lack of essential electron density delocalization between basins forming new bonds.

When the sequences of catastrophes (Figures 1 and 3) obtained for **BD**/**Acr** and **BD**/**Acr**···BH_3 reactions are analyzed, an interesting question arises: why the double $C_5=C_6$ bond in **Acr** is "reduced" to single bond before the double $C_1=C_2$ and $C_3=C_4$ bonds are "reduced" in **BD**? An answer stems from the catastrophe theory, which, as presented in Figure S1, shows that in the cusp catastrophe two maxima and one minimum are annihilated and new maximum is formed. From the universal unfolding of the cusp catastrophe (eq S3), one can obtain the parameter u, which determines the critical point nature at x = 0 with the Hessian matrix eigenvalue sign determining the type of catastrophe. The smaller this eigenvalue is, the sooner the cusp catastrophe occurs on the reaction path. In the isolated species, the positive eigenvalues of the relevant critical points of index one are: 0.059 for **BD**, 0.052 for **Acr**, 0.051 ($C_1=C_2$) and 0.015 ($C_3=C_4$) for the **PDA** and 0.076 for the **MVE**, respectively. These values are consistent with observed order of double bond reductions: in all cases, double bond corresponding to the smallest eigenvalue, is reduced first.

Apart from topological considerations we can suggest another explanation why in the case of the NED-DA reactions, the $C_1=C_2$ bond is "reduced" first in **BD**. An electron density redistribution in the "ring effect" proceeds both in the $V(C_1,C_2) \rightarrow V(C_2,C_3) \leftarrow V(C_3,C_4)$ direction and from $V(C_1,C_2)$ to the intermolecular region $C_1\cdots C_6$. Geometry rearrangements at the beginning of reactions favors electron flux to the $C_1\cdots C_6$ region over the one to the $C_4\cdots C_5$ region. An electron density depletion in the $C_1=C_2$ bond is therefore larger than in $C_3=C_4$ and presumably results in a decreasing a value of ELF and the catastrophe. Figure 12 presents a plot of $\eta(\mathbf{r})$ values versus the electron density ($\rho(\mathbf{r})$) for the **BD**/**Acr**···BH_3 reaction. It can be seen that increasing concentration of the electron density leads to larger ELF values, although small electron density values does not generally correspond with small values of ELF. In the case of the IED-DA reactions, "reductions" order for double bonds in **PDA** is reversed and $C_3=C_4$ is "reduced" before $C_1=C_2$. Due to an electron-withdrawing −CHO group presence in **PDA** and electron-releasing $-OCH_3$ group in **MVE**, electron flux is expected from dienophile to diene. Along with large "ring effect", strong "side chain effect" is also observed in **PDA** and the electron density is additionally withdrawn from the $C_3=C_4$ bond by the −CHO group. Thus, more effective depopulation in $C_3=C_4$ than in $C_1=C_2$ leads to a smaller amount of $\rho(\mathbf{r})$ in the bond and the cusp catastrophe.

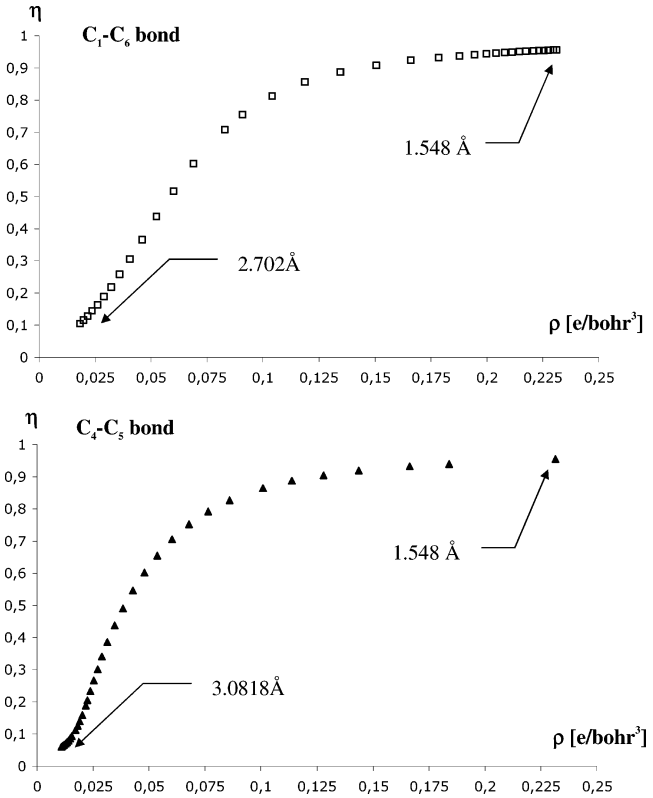

Figure 12. Dependence between values of the electron localization function $\eta(\mathbf{r})$ and electron density $\rho(\mathbf{r})$ calculated for the critical point of index 1 localized between C_1, C_6 and C_4, C_5 atoms for selected points on the IRC path in the reaction between 1,3-butadiene and acrolein catalyzed by BH_3.

III. Conclusions

The bonding evolution theory (BET) has been used to study the electron-pair reorganization, associated with bond breaking/forming processes along the reaction pathway. The normal electron demand Diels−Alder (NED-DA) reactions between butadiene (**BD**) and acrolein (**Acr**), and inverse electron demand Diels−Alder (IED-DA) reactions between 2,4-pentadienal (**PDA**) and methyl vinyl ether (**MVE**) have been investigated. The main conclusions can be summarized as follows:

(i) The molecular mechanism of these reactions consist of (1) "reduction" of double C_i═C_j bonds to single C_i−C_j bonds, (2) concentration of nonbonding electron density in monosynaptic basins V(C_i), (3) formation of single C_i−C_j bonds, and (4) formation of the double bond C_2═C_3.

(ii) In light of topological analysis there is not significant evidence for reactions to follow the asynchronous concerted mechanism where both intermolecular bonds are partially formed in TS. The BET reveals that first the C_1−C_6 bond is formed and subsequently the second C_4−C_5 bond is established.

(iii) Only two types of the catastrophes are observed: the fold, which yields the monosynaptic basins V(C_i) with the nonbonding electron density, and the cusp, leading to formation or annihilation of single/double bonds.

(iv) In the transition states for the **BD/Acr**, **BD/Acr**···BH_3 and **PDA/MVE** reactions, the monosynaptic basins V(C_i) are observed. This reflects nonbonding electron density concentration (on carbon atoms) in the region of the new C_1···C_6 bond. In the IED-DA reaction **PDA**···BH_3/**MVE**, the V(C_1,C_6) bonding basin is already formed in TS.

(v) The "new" double C_2═C_3 bond is formed before C_4−C_5 bond formation

(vi) First "reduction" of the double C_i═C_j bond occurs for different reactants in the cases of both NED- and the IED-DA reactions. These are **Acr** (NED) and **PDA** (IED), respectively. This is associated with different directions of the electron flux between the diene and dienophile and can also be predicted on the basis of topological arguments.

(vii) The electron redistribution during reaction can be seen as two mutual effects: large and regular "ring effect" associated with electron flux within the six-membered ring and smaller and irregular "side chain effect" appearing in the substituents.

(viii) The presence of the LA catalyst (BH_3) is reflected by BET as qualitatively different ELF topologies at the same point of uncatalyzed and catalyzed reactions. Formation of the C_1−C_6 bond in the catalyzed processes is more advanced than in the uncatalyzed case. An amount of the electron density required to form the V(C_1,C_6) and V(C_4,C_5) basins is smaller for the catalyzed reactions.

(ix) In the framework of the BET methodology, we suggest to substitute the arrow, a symbol used typically in chemical equations (A → B), by the much more informative catastrophe sequence: A: catastrophe sequence :B.

Acknowledgment. Dr. Agnieszka J. Gordon is kindly acknowledged for commenting, editing and proofreading the manuscript. This work was supported by research funds provided by the Ministerio de Educación y Cultura of the Spanish Government by DGICYT, projects BQU2003-04168-C03-03 and BQU2002-01032, and by Universitat Jaume I-Fundacio Bancaixa, Project P1B99-02. We thank the Servei d'Informatica, Universitat Jaume I and Wroclaw Centre for Networking and Supercomputing for generous allocation of computer time. The Marie Curie Development Host Fellowship program supported the work of S.B., contract no. HPMD-CT-2000-00055. The authors are solely responsible for the information communicated and it does not represent the opinion of The European Community. The European Community is not responsible for any use that might be made of data appearing therein.

Supporting Information Available: Computational details are summarized (S1). The catastrophe theory and the ELF topological analysis are presented in S2 and S3. This material is available free of charge via the Internet at http://pubs.acs.org.

References and Notes

(1) Krokidis, X.; Noury, S.; Silvi, B. *J. Phys. Chem. A* **1997**, *101*, 7277. Krokidis, X.; Silvi, B.; Alikhani, M. E. *Chem. Phys. Lett.* **1998**, *292*, 35. Krokidis, X.; Silvi, B.; Dezarnaud-Dandine, C.; Sevin, A. *New J. Chem.* **1998**, *22*, 1341. Krokidis, X.; Vuilleumier, R.; Borgis, D.; Silvi, B. *Mol. Phys.* **1999**, *96*, 265.

(2) Becke, A. D.; Edgecombe, K. E. *J. Chem. Phys.* **1990**, *92*, 5397. Silvi, B.; Savin, A. *Nature (London)* **1994**, *371*, 683. Savin, A.; Silvi, B.; Colonna, F. *Can. J. Chem.* **1996**, *74*, 1088. Silvi, B. *J. Mol. Struct.* **2002**, *614*, 3.

(3) Thom, R. *Stabilité Structurelle et Morphogénèse*; Intereditions: Paris, 1972.

(4) Berski, S.; Andrés, J.; Silvi, B.; Domingo, L. R. *J. Phys. Chem. A* **2003**, *107*, 6014.

(5) Polo, V.; Andres, J.; Castillo, R.; Berski, S.; Silvi, B. *Chem.−Eur. J.* **2004**, *10*, 5165.

(6) Santos, J. C.; Andres, J.; Aizman, A.; Fuentealba, P.; Polo, V. *J. Phys. Chem. A* **2005**, *109*, 3687.

(7) Santos, J. C.; Polo, V.; Andres, J. *Chem. Phys. Lett.* **2005**, *406*, 393.

(8) Polo V.; Andrés, J. *J. Comput. Chem.* **2005**, *26*, 1427.

(9) Fukui, K. *J. Phys. Chem.* **1970**, *74*, 4161. González, C.; Schlegel, H. B. *J. Phys. Chem.* **1990**, *94*, 5523.

(10) Diels, O.; Alder, K. *Justus Liebigs Ann. Chem.* **1928**, *460*, 98.

(11) Woodward, R. B.; Hoffmann, R. *Angew. Chem., Int. Ed. Engl.* **1969**, *8*, 781.

(12) Winkler, J. D. *Chem. Rev.* **1996**, *96*, 167.

(13) Carruthers, W. *Some Modern Methods of Organic Synthesis*, 2nd ed.; Cambridge University Press: Cambridge, U.K., 1978.

(14) Carruthers, W. *Cycloaddition Reactions in Organic Synthesis*; Pergamon: Oxford, U.K., 1990.

(15) Chen, Z.; Trudell, M. L. *Chem. Rev.* **1996**, *96*, 1179.

(16) Finguelli, F.; Tatichi, A. *The Diels−Alder reaction. Selected Practical Methods*; Wiley: New York, 2002.

(17) Evans, M. G. *Trans. Faraday Soc.* **1939**, *31*, 875.

(18) Sauer, J. *Angew. Chem., Int., Ed. Engl.* **1966**, *5*, 211. Sauer, J.; Sustmann, R. *Angew. Chem. Int. Ed. Engl.* **1980**, *19*, 779.

(19) Sauer, J. *Angew. Chem., Int., Ed. Engl.* **1967**, *6*, 16.

(20) Dewar, M. J. S.; Olivella, S.; Stewart, J. J. P. *J. Am. Chem. Soc.* **1986**, *108*, 5771.

(21) Wiest, O.; Montiel, D. C.; Houk, K. N. *J. Phys. Chem. A* **1997**, *101*, 8378. Houk, K. N.; Beno, B. R.; Nendel, M.; Black, K.; Yoo, H. Y.; Wilsey, S.; Lee, J. K. *THEOCHEM* **1997**, *398*, 169. Hrovat, D. A.; Beno, B. R.; Lange, H.; Yoo, H.-Y.; Houk, K. N.; Borden, W. T. *J. Am. Chem. Soc.* **2000**, *122*, 7456. Houk, K. N.; González, J.; Li, Y. *Acc. Chem. Res.* **1995**, *28*, 81.

(22) Diau, E. W.-G.; De Feyter, S.; Zewail, A. H. *Chem. Phys. Lett.* **1999**, *304*, 134.

(23) Weber, J. *Org. Lett.* **2003**, *5*, 1127.

(24) Sakai, S. *J. Phys. Chem. A* **2000**, *104*, 922.

(25) Breslow, R. *Acc. Chem. Res.* **1991**, *24*, 159.

(26) Fleming, I. *Frontier Orbitals and Organic Chemical Reactions*; John Wiley & Sons: New York, 1976; Chapter 4.

(27) Houk, K. N.; Li, Y.; Evanseck, J. D. *Angew. Chem., Int. Ed. Engl.* **1992**, *31*, 682.

(28) Kupeżyk-Subotkowska, L.; Shine, H. J. *J. Am. Chem. Soc.* **1993**, *115*, 5296.

(29) Storer, J. W.; Raimondi, L.; Houk, K. N. *J. Am. Chem. Soc.* **1994**, *116*, 9675.

(30) Gassman, P. G.; Gorman, D. B. *J. Am. Chem. Soc.* **1990**, *112*, 8624.

(31) Sustmann, R.; Rogge, M.; Nüchter, U.; Harvey, J. *Chem. Ber.-Recueil.* **1992**, *125*, 1665.

(32) Sustmann, R.; Tappanchai, S.; Bandmann, H. *J. Am. Chem. Soc.* **1996**, *118*, 12555.

(33) Birney, D. M.; Houk, K. N. *J. Am. Chem. Soc.* **1990**, *112*, 4127.

(34) García, J. I.; Martínez-Merino, V.; Mayoral, J. A.; Salvatella, L. *J. Am. Chem. Soc.* **1998**, *120*, 2415.

(35) Bader, R. F. W. *Atoms in Molecules: A Quantum Theory*; Oxford University Press: Oxford, U.K., 1994.